Romanian Journal of Mathematics and Computer Science
available online at https://rjm-cs.utcb.ro
Issue 2, Vol. 15 (2025)

Proceedings of the International Conference Riemannian Geometry and Applications - RIGA 2025
Bucharest, Romania, May 23-25, 2025

RED BLOOD CELLS AS HELFRICH SURFACES WITH SPHERICAL TOPOLOGY

EUGENIO AULISA, STONE FIELDS AND MAGDALENA TODA

Abstract. The paper analyzes Helfrich Surfaces with spherical topology and their corresponding shape equations. In particular, spheres and biconcave discoids are being presented as related to shapes of red blood cell.

Mathematics Subject Classification (2020): 35A05, 35G20, 49S05.
Key words: Helfrich surface, elastic surface, curvature functional, red blood cell, lipid bilayers.

Article history:
Received: July 3, 2025
Received in revised form: July 27, 2025
Accepted: July 28, 2025

1. Introduction

The past two decades have brought an increased interest in finding a suitable geometric model of the human *red blood cell* (abbreviated as RBC, and known under several names, of which *erythrocytes* is the prevalent one in the medical literature).

Achieving a precise shape model for red blood cells (RBCs) necessitates a multidisciplinary approach. This involves the theoretical frameworks of surface theory and calculus of variations, alongside robust computational analysis and empirical validation through advanced biophysical measurements using sophisticated instrumentation.

The elasticity theory of lipid bilayers, introduced by Canham and Helfrich in the early 1970s and further developed by Evans (see [8], [9]), models the equilibrium shapes of these membranes based on the principle of minimizing elastic free energy. This elastic energy, often referred to as the Helfrich-Canham energy, is represented as a curvature functional that depends on the mean curvature, Gaussian curvature, and other physical parameters of the bilayer surface. The mean curvature reflects the average local bending of the surface, while the Gaussian curvature describes its intrinsic curvature, independent of its embedding in space. Minimizing this energy functional allows researchers to predict and understand the diverse shapes that biological membranes, such as red blood cells, can take.

In [1], the sectional profile of the red blood cell (RBC) is studied in terms of Cassinian ovals, and estimates are provided for area, volume, area-to-volume ratio, total energy and other parameters. In [12], the shape of the RBC is obtained from the minimization of what is referred to as total elastic surface energy. It has been suggested that Cassini ovals [1] are the "most precise description" for the shape of the red blood cell. However, it was not mathematically verified if Cassini ovals actually satisfy the Shape Equation associated with the Helfrich-Canham functional. In a separate study, the authors of the present work proved that Cassini ovals do not constitute actual solutions for the Helfrich-Canham shape equation, except for the round sphere which represents a limit case. The current study analyzes the Helfrich-Canham Shape Equation, with the red blood cell as a primary application.

Under normal circumstances, human red blood cells (RBCs) have a specific biconcave disc shape, which enables optimal flexibility and surface area for efficient oxygen transport. However, under certain conditions, red blood cells can take the shape of round spheres. That may happen in some disorders like the following:

a) *Hereditary Spherocytosis*: This inherited blood disorder affects the red blood cell membrane, leading to cells that are more fragile and sphere-shaped, known as spherocytes. These cells are less flexible and prone to breaking down prematurely (*hemolytic anemia*).

b) *In Vitro Conditions*: Experiments have shown that red blood cells can be induced to adopt a spherical shape in specific laboratory settings, such as when their ATP is depleted or when exposed to certain chemicals or compounds.

The prevalent cases discussed in this paper are the round spheres and biconcave discoids.

2. First Variation

In the goal of modeling the geometry of the red blood cell (RBC) we will be considering the surface energy functional

$$\Theta(M) = \iint_M \beta(2H - c_0)^2 \, dS + \lambda \int dA + \Delta P \int dV.$$

which is called the Helfrich-Canham functional. Here $\beta > 0$ represents the bending rigidity, and $c_0 \in \mathbb{R}$, where c_0 is called the *spontaneous curvature* in [8], [9] and other related works. It is important to mention that c_0 may have different signs for different real-world models. The function $H = -\frac{k_1+k_2}{2}$ is alternatively called the *mean curvature* or *Germain curvature* of the immersion. Its sign as a function depends on the surface orientation. We would like to remark that λ (*surface tension*) and ΔP (*osmotic pressure*) are two Lagrange multipliers corresponding to area and volume constraints, respectively.

It is important to note that some papers consider a slightly different Helfrich integral, whose first integrand would be $(H-c_0)^2$ instead of $(2H-c_0)^2$, but we adopt the definition introduced by [15], [10], [8]. Thus, notations of various papers may also differ on the definition of spontaneous curvature c_0, by a factor of 2.

If $c_0 = 0$, the functional corresponds to the classical Willmore functional, whose critical surfaces are known to be Willmore surfaces.

One first step for researchers working in this field was to calculate the first variation in the normal direction of a one-parameter family of surfaces. Since this surface is closed, one can use Green's Theorem to obtain the corresponding Euler-Lagrange PDE, an approach that we have employed as well. It follows that the critical points of the curvature functional must satisfy the following Euler-Lagrange equation corresponding to the Helfrich-Canham functional, which is

referred to in the literature as *Shape Equation*, *Helfrich Equation* or *Helfrich Shape Equation* ([15], [10], [8], [9], [11], [6]):

$$2\Delta H + (2H - c_0)[2H^2 - 2K + c_0 H] + \bar{P} - 2\bar{\lambda}H = 0, \tag{2.1}$$

where $\bar{P} := \Delta P/\beta$ and $\bar{\lambda} := \lambda/\beta$.

The $\bar{P}$, $\bar{\lambda}$ notations above are very useful, unless we consider the rigidity factor $\beta = 1$, as some articles do.

It is known that (2.1) is a fourth order nonlinear elliptic partial differential equation, which can be very difficult to work with analytically.

3. Shape Equation for the particular case of Axisymmetric Surfaces with Spherical Topology

Let $X : D \to \mathbb{R}^3$ be a surface immersion in $\mathbb{R}^3$. Here D denotes an open, simply connected domain immersed in $\mathbb{R}^3$ where $D = (0, \alpha) \times (0, 2\pi)$, and X depends on two parameters s, v such that

$$X = X(s, v) = (r(s)\cos v, r(s)\sin v, z(s)).$$

The parameter s is the arclength of the profile curve $(r(s), z(s))$, which generates the surface of revolution X by revolving around the z-axis. Such a surface of revolution will be called an *axisymmetric surface*. We shall study a cell whose shape is represented by such a closed surface, where s, r and ψ are the arc length of the profile curve, the radius and the angle between the horizontal and the profile curve, respectively. Thus, the profile can actually be parameterized as a function $\psi = \psi(r)$, where r represents the rotation radius of some point in the contour line, while ψ is the tangent angle of the contour line at that point. By definition, the angle $\psi(r)$ must satisfy the condition

$$\psi(r) = -\arctan\frac{dz}{dr}. \tag{3.1}$$

Here, the coordinate functions as functions of arclength are $z(s)$ and $r(s)$ and satisfy the following expressions:

$$\frac{dz}{ds} = -\sin\psi; \qquad \frac{dr}{ds} = \cos\psi, \tag{3.2}$$

which is equivalent to

$$\frac{dz}{dr} = -\tan\psi. \tag{3.3}$$

Note that the signs of these expressions are compatible with the angle orientation which is fixed in our case. In the corresponding Figure 1, the angle ψ is measured from the tangent to the horizontal line, in the trigonometric sense.

These equations follow from (3.1).

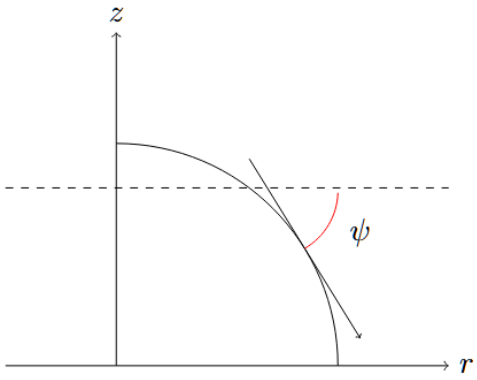

Figure 1. Profile of a surface of revolution satisfying a shape equation

Using this new frame, it is possible to transform the Euler-Lagrange equation using reformulations of the curvatures. Using calculations from [10], we consider the modified mean and Gaussian curvatures along the profile curve $z(r)$,

$$H = -\frac{k_1 + k_2}{2} = -\frac{1}{2}(\cos\psi(\frac{d\psi}{dr}) + \frac{\sin\psi}{r}), \tag{3.4}$$

$$K = k_1 k_2 = \cos(\psi)\sin(\psi)\frac{1}{r}\frac{d\psi}{dr}. \tag{3.5}$$

Here, as before, $\psi(s)$ represents the angle between the tangent line of the profile curve $(x(s), z(s))$ and the xy-plane.

In a similar manner to [15], we obtained the following *Helfrich Shape Equation*:

$$0 = \mathcal{H} = -\cos^3\psi\frac{d^3\psi}{dr^3} + 4\sin\psi\cos^2\psi\frac{d^2\psi}{dr^2} - cos\psi(\sin^2\psi - \frac{1}{2}\cos^2\psi)\left(\frac{d\psi}{dr}\right)^3 + \frac{7\sin\psi\cos^2\psi}{2r}\left(\frac{d\psi}{dr}\right)^2.$$

For the convenience of our computations, $\mathcal{H}$ denotes the entire trigonometric expression above, which can be further developed as

$$\mathcal{H} = -\frac{2\cos^3\psi}{r}\frac{d^2\psi}{dr^2} + \left(\frac{c_o^2}{2} - \frac{2c_o\sin\psi}{r} + \frac{\sin^2\psi}{2r^2} + \bar{\lambda} - \frac{\sin^2\psi - \cos^2\psi}{r^2}\right)\cos\psi\frac{d\psi}{dr}$$

$$+\bar{P} + \bar{\lambda}\sin\psi - \frac{\sin^2\psi}{2r^3} + \frac{c_o^2\sin\psi}{2r} - \frac{\sin\psi\cos^2\psi}{r^3}.$$

In the particular case of axisymmetric surfaces that are topologically equivalent to spheres, the previous equation reduces to the following *Axisymmetric Shape Equation*:

$$0 = \mathcal{H} = \cos^2\psi\frac{d^2\psi}{dr^2} - \frac{\sin\psi\cos\psi}{2}(\frac{d\psi}{dr})^2 - \frac{\sin\psi}{2r^2 cos\psi} - \frac{\sin\psi\cos\psi}{2r^2} - \frac{c_0^2\sin\psi}{2\cos\psi} \tag{3.6}$$

$$+\frac{\cos^2\psi}{r}\frac{d\psi}{dr} - \frac{c_0\sin^2\psi}{r\cos\psi} - \frac{\bar{P}}{2}\frac{r}{\cos\psi} - \bar{\lambda}\frac{\sin\psi}{\cos\psi}.$$

For the prerequisites necessary to reach this equation, one may check [10] and [11].

Remark 3.1. It is interesting to point out that [15] and [10] both discuss the critical points of Helfrich type energies. While we will not repeat their arguments, it is important to clarify that [10] use Lagrange multipliers for the two given constraints below

$$\frac{dz}{ds} = -\sin\psi; \qquad \frac{dr}{ds} = \cos\psi. \tag{3.7}$$

Namely, they added the following terms to the usual Lagrangian

$$\eta(\frac{dz}{ds} + \sin\psi) + \gamma(\frac{dr}{ds} - \cos\psi).$$

On the other hand, [15] used a different way to extend the Lagrangian, namely by adding a single term to the integrand inside the functional:

$$\eta(\frac{dz}{dr}\cos\psi + \sin\psi).$$

3.1. **The Case of Round Spheres as Solutions to the Shape Equation.**

The simplest way to obtain the shape equation for the sphere of radius a is to replace $k_1 = k_2 = H = 1/a$ or $k_1 = k_2 = H = -1/a$ (for its two opposite orientations) directly into the Helfrich Shape Equation $2\Delta H + (2H - c_0)[2H^2 - 2K + c_0 H] + \bar{P} - 2\bar{\lambda}H = 0$.

This procedure will result in the necessary and sufficient conditions $\bar{P}a^2 - [c_0^2 + 2\bar{\lambda}]a + 2c_0 = 0$, and $\bar{P}a^2 + [c_0^2 + 2\bar{\lambda}]a + 2c_0 = 0$, respectively.

However, we may choose to verify the function $\psi = \arcsin r$, and its opposite, directly into the axisymmetric shape equation that explicitely depends on ψ.

Theorem 3.2. *For $\psi = a\arcsin r$, in order for spherical solutions to exist, the surface Σ must satisfy the following constraint on the parameters c_0, $\bar{P}$, $\bar{\lambda}$:*

$$\bar{P}a^2 + [c_0^2 + 2\bar{\lambda}]a + 2c_0 = 0 \tag{3.8}$$

Proof. The process of replacing ψ directly in the shape equation is tedious, but straightforward. Requiring that $\psi = a\arcsin r$ satisfies the axisymmetric shape equation, one obtains some very long expressions that are not easily simplified by any mathematical software. However, after careful regrouping, manipulations, and cancellations, we obtain the constraint above in its simplest form.

It would first be easiest to see the process for the case $a = 1$. We use $\frac{dz}{dr} = -\tan\psi$ by definition of ψ, and, from (3.7), $\frac{dz}{ds} = -\sin\psi$ and $\frac{dr}{ds} = \cos\psi$. Differentiating ψ with respect to r, it follows that $\frac{d\psi}{dr} = (1-r^2)^{-\frac{1}{2}}$ and furthermore $\frac{d^2\psi}{dr^2} = \frac{r}{(1-r^2)^{\frac{3}{2}}}$. We will now modify the shape equation with respect to this constraint on the angle ψ. Substituting these expressions, we obtain

$$\mathcal{H} = (1-r^2)\frac{r}{(1-r^2)^{\frac{3}{2}}} - \frac{r\sqrt{1-r^2}}{2}\frac{1}{1-r^2} - \frac{1}{2r\sqrt{1-r^2}} - \frac{r\sqrt{1-r^2}}{2r^2} - \frac{c_0^2}{2}\frac{r}{\sqrt{1-r^2}}$$
$$+\frac{1-r^2}{r}\frac{1}{\sqrt{1-r^2}} - \frac{c_0 r^2}{r\sqrt{1-r^2}} - \frac{\bar{P}r}{2\sqrt{1-r^2}} - \bar{\lambda}\frac{r}{\sqrt{1-r^2}} = 0.$$

Following a brief simplification and multiplying everything by $\sqrt{1-r^2} > 0$, we have that

$$r - \frac{r}{2} - \frac{1}{2r} - \frac{1-r^2}{2r} - \frac{c_0^2 r}{2} + \frac{1-r^2}{r} - c_0 r - r(\frac{\bar{P}}{2} + \bar{\lambda}) = 0.$$

Some terms that depend on r cancel out, resulting in the following expression:

$$-r\frac{c_0^2}{2} - c_0 r - r(\frac{\bar{P}}{2} + \bar{\lambda}) = 0.$$

This is significant: in order for the unit sphere to be a solution, this condition must be satisfied entirely by parameters $c_0, \bar{P}$ and $\bar{\lambda}$.

Likewise, in order for the sphere of radius r to be a solution to the Helfrich equation, we can substitute the function $\psi = a \arcsin r$ in the shape equation, and we obtain the more general condition in terms of the radius a:

$$a^2\frac{c_0^2}{2} + ac_0 + a^3\frac{\bar{P}}{2} + a^2\bar{\lambda} = 0, \tag{3.9}$$

which, after simplifications, can be rewritten as

$$\bar{P}a^2 + [c_0^2 + 2\bar{\lambda}]a + 2c_0 = 0 \tag{3.10}$$

where a is the radius of the round sphere.

□

Symmetrically, we obtain

Theorem 3.3. *For $\psi = -a \arcsin r$, in order for spherical solutions to exist, the surface Σ must satisfy the following constraint on the parameters c_0, $\bar{P}$, $\bar{\lambda}$:*

$$\bar{P}a^2 - [c_0^2 + 2\bar{\lambda}]a + 2c_0 = 0. \tag{3.11}$$

Thus, we have two symmetric solutions that correspond to different conditions on the pressure, spontaneous curvature and tension. Since $\psi(r)$, $\psi'(r)$ and $\psi''(r)$ will all be changing sign, along with $\sin\psi$ changing sign and $\cos\psi$ remaining invariant with respect to the change $\psi \to -\psi$, we see that the shape equation

$$\bar{P}a^2 + [c_0^2 + 2\bar{\lambda}]a + 2c_0 = 0 \tag{3.12}$$

changes to

$$-\bar{P}a^2 + [c_0^2 + 2\bar{\lambda}]a - 2c_0 = 0, \tag{3.13}$$

which would physically correspond to a sign change for the spontaneous curvature and a sign change in the pressure difference alike.

For the sake of completion, both solutions must be taken into account, as the spontaneous curvature and pressure may be considered positive or negative and are not a priori prescribed. This is an important consideration, which other studies did not discuss.

4. Biconcave Discoids: Suitable Versus Unsuitable Models for the RBC

We would like to point out that the profile $\psi(r) = \arcsin[r(c_0(\ln r + b)]$, which was found by some previous authors ([9]), is not among the solutions we have found or presented. There are multiple possible reasons for that. As [15] shows, this type of solution with $\Delta P = \lambda = 0$ and $c_0 < 0$, which was proposed for the red blood cell by some papers, is not adept for a physical model like the red blood cell.

Additionally, assuming that such a model would exist, as [15] stated, the only possibility for the shape equation $\mathcal{H} = 0$ to be satisfied would be for the spontaneous curvature c_0 to be zero, which is not the case for an authentic red blood cell model.

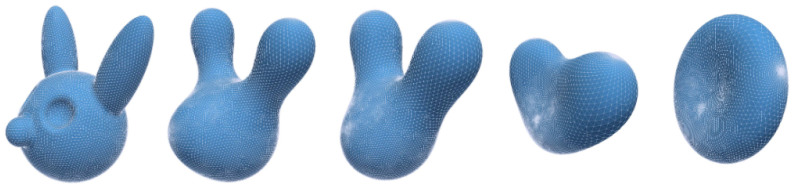

FIGURE 2. Willmore flow converging to a biconcave discoid as energy minimizer under joint area and volume constraints

Moreover, as [15] explains, if the spontaneous curvature were non-zero, then the profile $\psi(r) = \arcsin[r(c_0(\ln r + b)]$ would have a local extreme value exactly at $r = e^{(-b/c_0)}$, which means the angle ψ could not vary independently. Another important remark is that such a profile would lack C^2 regularity at the points of the z-axis of the profile.

4.1. **Computational Willmore flow converging to biconcave discoids under joint area and volume constraints.** We would now want to attract attention to a gradient Willmore flow under *simultaneous area and volume constraints*, which are both mandatory in order for the flow to converge to the biconcave discoid model.

Through specific computational algorithms that were employed by the first author, certain coupled PDE systems were solved using finite element methods along with automatic differentiation methods, in order to produce numerical solutions to the Willmore flow equation by [4]. The Figure 2 represents a regular ($p = 2$) Willmore surface evolution of a closed surface membrane model with 18k triangles, constrained by both surface area and enclosed volume. If an area constraint or a volume constraint (but not both) would be prescribed, then the closed cell in the picture would become a globally-minimizing round sphere, instead of a biconcave discoid shape like the red blood cell.

We remark the biconcave discoid shape characteristic of genus 0 minimizers of the constrained Helfrich-Canham energy such as red blood cells.

It is further remarkable that the flow behavior here is different than the case when either the volume or area constraint is considered on its own.

4.2. **Recent advances in the red blood cell shape.** Under the assumption that the bending energy density of the red blood cell (RBC) surface is proportional to the average square of the adjusted normal curvature in all the directions at every point, $\langle(\kappa - \mathring{\kappa})^2\rangle$, and that this bending energy density is constant everywhere, the authors of [6] (including the last author of the present article) found the differential equations which characterize the RBC profiles. Since this differential equation is of second degree in the first derivative, two separate solutions were found by the authors. Moreover, the RBC profile was shown to be the union of both solutions at an inflection point in such a way that the two solutions extend each other regularly.

The first solution has a slope increasing from zero at the RBC center as the radial coordinate goes towards the inflection point, while the second solution has a decreasing slope from the inflection point up to the outer radius of the RBC model. At the inflection point, the slopes of both solutions are the same. The team showed that the resulting surface profile is always regular.

Further, the authors computed the RBC profiles without spontaneous curvature ($c_0 = 0$) and with spontaneous curvature c_0 nonzero, respectively, as two separate cases. It was then shown

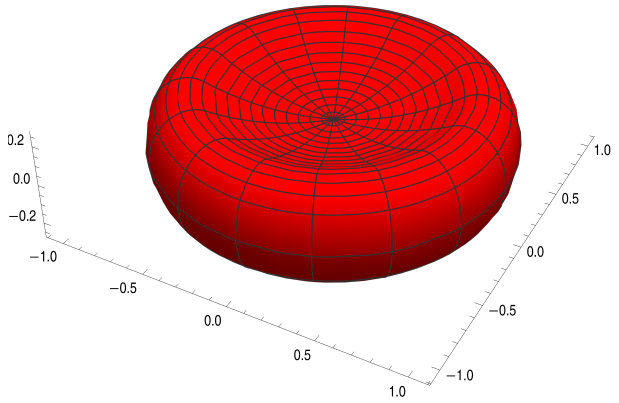

Figure 3. Red Blood Cell obtained in [6] through Variational and ODE Methods

that the first case (i.e., the Willmore surface case) cannot fit the actual RBC shape, whereas the second case agrees well with the observed RBC geometric parameters. Thus, it was shown that the Helfrich biconcave discoid that best fits the red blood cell shape is always a regular surface with nonzero spontaneous curvature, which was evaluated in [6] and led to a proper RBC profile model as seen in the Figure 3.

The authors analyzed the variational problem in a rigorous and complete manner. For this study, it was mathematically and physically essential to assume that the bending energy density is proportional to the square of the adjusted mean curvature.

Observation: One interesting fact to point out is that profile curves that satisfy the shape equation (3.6) do not necessarily imply that surfaces generated from such curves represent minimizers of Helfrich energy. Another work from [14] recently studied other closed Helfrich surfaces. They remarked that some family of axisymmetric Helfrich closed surfaces is characterized by a mean curvature that is constant, while another one satisfies the *reduced membrane equation*

$$H + c_0 = -\frac{\nu_3}{z}.$$

However, as observed, the biconcave discs fall into neither of the categories above. Thus, our studies do not properly intersect with [14].

It is important to note that the RBC model represents a Helfrich regular surface in the sense that it admits a tangent plane at each point. Some of the singularities at $r = 0$ points are artificially introduced by considering parameterizations that depend on the logarithmic function $\ln r$.

5. Cassini Ovals are not Helfrich Surfaces, but can mimic them

Here, we will introduce the Cassini ovals (see Figure 4), proposed as a family of curves that best fit the red blood cell, as previously mentioned [1]. The Cassini ovals are thought to be a generalization of the lemniscate. We define the Cassini ovals in the following form

$$z(r) = \pm\sqrt{\sqrt{4a^2r^2 + c^4} - a^2 - r^2},$$

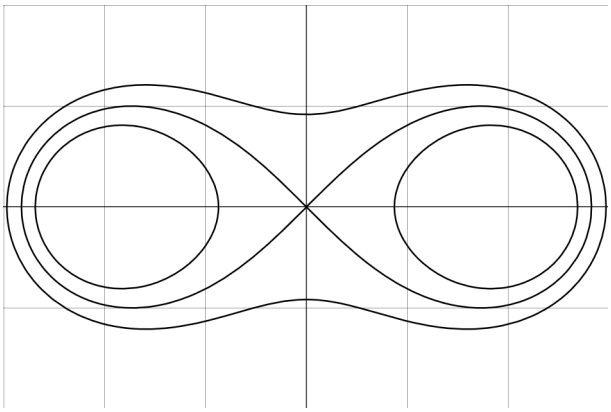

Figure 4. Cassini ovals

where a and c are real-valued constants that compose certain characteristics of the Cassini ovals. We call $\epsilon = \frac{a}{c}$ the biconcavity and $e = \frac{c}{a}$ the eccentricity of the Cassini ovals.

Up to rescaling, we can rewrite the equation as

$$z(r) = \pm\sqrt{\sqrt{4\epsilon^2 r^2 + 1} - \epsilon^2 - r^2}. \tag{5.1}$$

Notice that for $0 \leq \epsilon < 1$ the argument under the outer square root

$$\sqrt{4\epsilon^2 r^2 + 1} - \epsilon^2 - r^2 \tag{5.2}$$

is nonnegative for $0 \leq r \leq \sqrt{1+\epsilon^2}$, and for $\epsilon \geq 1$ it is nonnegative for $\sqrt{-1+\epsilon^2} \leq r \leq \sqrt{1+\epsilon^2}$. Moreover, for the derivatives of $z(r)$ to exist, we need to restrict the domain further and assume the argument in Eq. (5.2) to be strictly positive. Then, for given $\epsilon \geq 0$ the domain of $z(r)$ is given by

$$D := \begin{cases} 0 \leq r < \sqrt{1+\epsilon^2} & \text{for} \quad 0 \leq \epsilon < 1, \\ \sqrt{-1+\epsilon^2} < r < \sqrt{1+\epsilon^2} & \text{for} \quad \epsilon \geq 1. \end{cases} \tag{5.3}$$

Based on this theoretical framework, we have recently proved the following result, whose proof can be found in [3].

Theorem 5.1. *For $\epsilon > 0$, Cassini ovals as a profile curve do not satisfy the shape equation* (3.6).

6. Conclusion and Open Problems

Outside of the case of round spheres, we found that no simple explicit solution $\psi(r)$ corresponds to an explicitely given profile of the red blood cell. In a separate paper [6], the last author of the current work presented some numerical solutions along with analytic solutions that cannot be written explicitly, but satisfy some specific differential equations, with a significant number of changes of variables and parametrization that involve both trigonometric and logarithmic functions. We presented numerical solutions that match the red blood cell experimental models.

Most known RBC models currently assume that the spontaneous curvature is a constant, based on the experimental measurements of the red blood cells. As such, it is possible to reframe spontaneous curvature as a smooth function. If bending energy density is assumed to be proportional to the average of the square of the adjusted normal curvature over all the directions

passing through this point for all points on the surface X, we define the specific elastic energy to be

$$\rho = \frac{1}{n}\sum_{i\in I}^{n}(k_i - c_0)^2.$$

It will be very interesting for the future to consider cases when the spontaneous curvature varies in time, thus creating a dynamical system of Helfrich solutions.

Acknowledgement. We would like to thank our colleague Erhan Güler for his suggestions regarding this work. The last author would like to thank the Simons Foundation for the financial support she has received as a Mathematics and Physical Sciences-Collaboration Grant for Mathematicians, entitled *Applications of Willmore Energy Functionals to Protein Biology*, Simons Award 632274, 2019-2025. No conflicts of interest exist for the current work.

References

[1] B. Angelov and I. Mladenov, *On the geometry of red blood cell,* Geom. Integrability & Quantization **1** (2000), 27-46.

[2] B. Athukorallage, G. Bornia, T. Paragoda and M. Toda, *Willmore-type energies and Willmore-type surfaces in space forms,* J. Geometry and Topology **18(2)** (2015), 93-108.

[3] E. Aulisa, S. Fields and M. Toda, *The geometry of red blood cells*, preprint, Research Project sponsored by the Simons Foundation (2025).

[4] E. Aulisa and A. Gruber, *Computational p-Willmore flow with conformal penalty*, ACM Trans. Graphics **22** (2019), 1-16.

[5] H.J. Deuling and W. Helfrich, *Red blood cell shapes as explained on the basis of curvature elasticity*, Biophys J. **16(8)**(1976), 861-869.

[6] R.C. Gonzalez, I. Mladenov and M. Toda, *On the shape of red blood cell*, J. Geometry and Symmetry in Physics **72** (2025), 1-38.

[7] A. Gruber, *Curvature Functionals and p-Willmore Energy*, Doctoral Dissertation, Texas Tech University. (2019).

[8] W. Helfrich, *Elastic properties of lipid bilayers: theory and possible experiments,* Zeitschrift für Naturforschung **28(11-12)** (1973), 693-703.

[9] H. Jian-Guo and O.Y. Zhong-Can, *Shape equations of the axisymmetric vesicles,* Physical Review **47(1)** (1993), 461-467.

[10] F. Jülicher and S.U. Seifert, *Shape equations for axisymmetric vesicles: a clarification,* Physical Review **49(5)** (1994), 4728-4731.

[11] G. Kumar, *Shape equations of the axisymmetric vesicles,* Research Project (2022).

[12] Q. Liu, Z. Haijun, J. Liu and O. Zhong-Can, *Spheres and prolate and oblate ellipsoids from an analytical solution of spontaneous curvature fluid membrane model*, Phys. Rev. **60** (1999), 3227-3233.

[13] J.C.C. Nitsche, *Lectures on Minimal Surfaces,* Translated from the German by J.M. Feinberg, Cambridge University Press **1** (1989).

[14] B. Palmer and A. Pampano, *Stability of Membranes*, https://arxiv.org/abs/2401.05285 (2024).

[15] N. Vaidya, H. Huang and S. Takagi, *Correct equilibrium shape equation of axisymmetric vesicles,* in C. Constanda, S. Potapenko (Eds.), *Integral Methods in Science and Engineering: Techniques and Applications*, MA Birkhäuser Boston (2008), 267-276.

Department of Mathematics and Statistics, Texas Tech University, Lubbock, TX, 79409, USA
Email address: eugenio.aulisa@ttu.edu, stofield@ttu.edu, magda.toda@ttu.edu